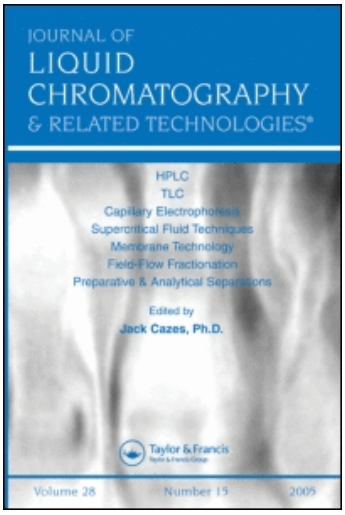

Journal of Liquid Chromatography & Related Technologies
Publication details, including instructions for authors and subscription information:
http://www.informaworld.com/smpp/title~content=t713597273

Separate Determination of Rate Constants from Reversible Reactions in a Chromatographic Column and Eluent Using Empirical Peak Shape Equations

Jana Lange[a]; Detlef Haberland[a]; Richard Thede[a]
[a] Institute of Chemistry and Biochemistry, University of Greifswald, Greifswald, Germany

Online publication date: 02 March 2003

To cite this Article Lange, Jana , Haberland, Detlef and Thede, Richard(2003) 'Separate Determination of Rate Constants from Reversible Reactions in a Chromatographic Column and Eluent Using Empirical Peak Shape Equations', Journal of Liquid Chromatography & Related Technologies, 26: 2, 285 — 296
To link to this Article: DOI: 10.1081/JLC-120017169
URL: http://dx.doi.org/10.1081/JLC-120017169

MARCEL DEKKER, INC. • 270 MADISON AVENUE • NEW YORK, NY 10016

JOURNAL OF LIQUID CHROMATOGRAPHY & RELATED TECHNOLOGIES®
Vol. 26, No. 2, pp. 285–296, 2003

Separate Determination of Rate Constants from Reversible Reactions in a Chromatographic Column and Eluent Using Empirical Peak Shape Equations

Jana Lange, Detlef Haberland, and Richard Thede*

Institute of Chemistry and Biochemistry, University of Greifswald, Greifswald, Germany

ABSTRACT

A new mathematical-analytical equation is derived for fitting purposes in the determination of mobile phase rate constants of enantiomerization from liquid chromatographic reactor experiments with a recycling of the internal chromatogram via an empty capillary. The equation was successfully tested with results from numerical calculations, as well as results from the on-column enantiomerization of oxazepam.

Key Words: Chromatographic reactor; Reversible reactions; Rate constants

*Correspondence: Richard Thede, Institute of Chemistry and Biochemistry, University of Greifswald, Soldmannstrasse 23, D-17489 Greifswald, Germany; E-mail: thede@uni-greifswald.de.

DOI: 10.1081/JLC-120017169 1082-6076 (Print); 1520-572X (Online)

SYMBOLS

c	concentration
$d^i_{mjRk}\ldots$	ith differential peak area, from the jth generation converted in the Rth (Roman number) part of the recycling setup into the kth generation
h_x	experimental recorder signal
h	theoretical recorder signal
k_a	dead-time related apparent rate constant
k_e	rate constant (mobile phase)
m_0	concentration-time area of reactant at the column inlet
t	time
t_E	residence time in the capillary
t_R	maximum retention time of the reactant in a recycling setup
t_P	maximum retention time of the product in a recycling setup
t_0	dead time
κ	retention-time related apparent rate constants
λ	reduced spatial coordinate
λ_i	reduced spatial coordinate of the capillary inlet
λ_o	reduced spatial coordinate of the capillary outlet
μ_R	maximum retention time of reactant (column)
μ_P	maximum retention time of product (column)
σ	standard deviation of differential product pulse
σ_R	standard deviation of reactant peak
σ_P	standard deviation of product peak
τ	retention ratio product vs. reactant (recycling setup)
τ_c	retention ratio product vs. reactant (column), selectivity

INTRODUCTION

Many papers have been published during the last decade on the determination of rate constants from the characteristic chromatograms due to reversible on-column-reactions, especially enantiomerizations (for a comprehensive review, see Ref.[1]). Often, methods are used, in which computer simulated chromatograms are fitted to experimental chromatograms, and normally, the authors start with the assumption of corresponding rate constants in the mobile and in the stationary phase. However, because of the principle of microkinetic reversibility[2] two different (however similar) on-column rate constants are estimated.

In a previous paper,[4] the usefulness of a so-called simulated recycling setup was shown for the separate determination of on-column and eluent rate constants from irreversible first order reactions. This setup, which was in the first place suggested by the Langer group,[3] consists of a separation column with the reduced length coordinates from 0 to λ_i, an empty HPLC capillary of at least 15 m with the reduced length coordinates from λ_i to λ_o, and another separation column like the first one with the reduced length coordinates from λ_o to 1.

Let us now consider a racemate, which is injected onto this setup (cf. Fig. 1), then the enantiomers are separated within the first column, and at the same time enantiomerization takes places producing a plateau of racemate between the pure enantiomers. No separation occurs within the capillary, and therefore the enantiomerization proceeds primarily under the peaks of the pure enantiomers. When passed into the final column, the same process as in the first column takes places except the fact that the product formed within the capillary is now separated from the pure enantiomers forming a so-called extra peak on the plateau between the pure enantiomers. Therefore, the extra peak contains the information about the reaction in the pure mobile phase, and the present paper reports on the derivation and application of an approximated analytical peak shape equation for the estimation of rate constants from such types of reaction chromatograms.

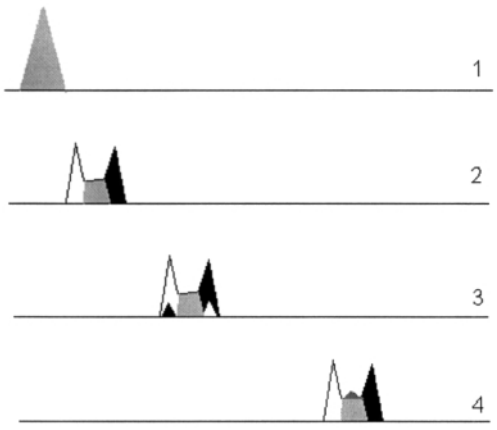

Figure 1. Development of a reaction chromatogram in a simulated recycling setup (Schematic). (1) Injection of racemate; (2) Chromatogram at the end of colum I; (3) Chromatogram at the end of the capillary; (4) Chromatogram at the end of the second column or the second run through the same column exhibiting the extra peak (Black: D-form, White: L-Form, Gray: racemate, Dark Gray: extra peak).

MATHEMATICAL MODELLING

The mathematic modelling is based on the assumptions from the model of linear, isothermal chromatography. The reversible reaction is approximated by consecutive reactions with alternate rate constants:

$$R \leftrightarrows P \approx R \rightarrow P \rightarrow R \rightarrow P \rightarrow R$$

Then, starting from the reactant R, differential pulses of a first generation P are produced at any cross section of the apparatus. Each one of these produces second order differential pulses of a first generation R, etc. Any of the differential pulses copies the shape of its parent at the point of conversion, but then moves with the speed and the peak spreading due to its own chromatographic parameters. However, one has to consider the segments of the recycling setup. Taking into account four generations, the following interconversions take place.

In the leading column (segment I):

$$m_0 \rightarrow dm_{0I1} \rightarrow d^2m_{0I1I2} \rightarrow d^3m_{0I1I2I3} \rightarrow d^4m_{0I1I2I3I4}$$

In the capillary (segment II):

$$m_0 \rightarrow dm_{0II1} \rightarrow d^2m_{0II1II2} \rightarrow d^3m_{0II1II2II3} \rightarrow d^4m_{0II1II2II3II4}$$
$$dm_{0I1} \rightarrow d^2m_{0I1II2} \rightarrow d^3m_{0I1II2II3} \rightarrow d^4m_{0I1II2II3II4}$$
$$d^2m_{0I1I2} \rightarrow d^3m_{0I1I2II3} \rightarrow d^4m_{0I1I2II3II4}$$
$$d^3m_{0I1I2I3} \rightarrow d^4m_{0I1I2I3II4}$$

After recycling or simulated recycling (segment III):

$$m_0 \rightarrow dm_{0III1} \rightarrow d^2m_{0III1III2} \rightarrow d^3m_{0III1III2III4} \rightarrow d^4m_{0III1III2III3III4}$$
$$dm_{0I1} \rightarrow d^2m_{0I1III2} \rightarrow d^3m_{0I1III2III3} \rightarrow d^4m_{0I1III2III3III4}$$
$$d^2m_{0I1I2} \rightarrow d^3m_{0I1I2III3} \rightarrow d^4m_{0I1I2III3III4}$$
$$d^3m_{0I1I2I3} \rightarrow d^4m_{0I1I2I3III4}$$
$$dm_{0II1} \rightarrow d^2m_{0II1III2} \rightarrow d^3m_{0II1III2III3} \rightarrow d^4_{0II1III2III3III4}$$
$$d^2m_{0I1III2} \rightarrow d^3m_{0II1II2III3} \rightarrow d^4m_{0II1II2III3III4}$$
$$d^3m_{0II1II2III3} \rightarrow d^4m_{0II1II2III3III4}$$
$$d^2m_{0I1II2} \rightarrow d^3m_{0I1II2III3} \rightarrow d^4m_{0I1II2III3III4}$$
$$d^3m_{0I1II2III3} \rightarrow d^4m_{0I1I2III3III4}$$

In general (for details see Ref.[6]), the differential concentration of a differential pulse is given by the relation:

$$d^n c = \frac{d^n m}{\prod_1^n d\lambda_i} \Psi(t, \lambda) \prod_1^n d\lambda_i \tag{1}$$

According to the reaction scheme given above, fourteen different peak types had to be considered, i.e., even the developed differential equations from Eq. (1) take several pages.

In the present paper, the peak shape function Ψ is assumed to be a Gaussian, but also an EMG function would be suitable. However, considerably skewed peaks are an indication for nonlinear isotherms with consequences to the precision of the rate constants determined. In a linear model, skew, excess, and standard deviations of the reactant peaks cannot be altered independently, and our simulations have shown that a difference between a Gaussian and a peak shape function, considering skew and excess, does not appear until no more separation is achieved.

The concentration from, i.e., the 4th generation of differential pulses is obtained from an integration following the scheme:

$$c = \int_{\lambda_{\text{beg}}}^{\lambda_1} \int_{\lambda_1}^{\lambda_2} \int_{\lambda_2}^{\lambda_3} \int_{\lambda_3}^{\lambda_{\text{end}}} \frac{d^4 m}{\prod_1^n d\lambda_i} \Psi(t, \lambda)\, d\lambda_4\, d\lambda_3\, d\lambda_2\, d\lambda_1 \tag{2}$$

Depending on the segment, λ_{beg} can be either 0, $\lambda_1$or λ_0, and λ_{end} can be either λ_i, λ_o or 1. Analytical integrations can only take place assuming standard deviations not depending on the spatial coordinate. In the present case, we choose a squared average of the reactant standard deviations to approximate the product pulse standard deviation, since the largest place between the reactant peaks is occupied by the extra peak (i.e., a sum of differential peaks having the same average standard deviation):

$$\sigma^2 \approx \frac{\sigma^2{}_R + \sigma^2{}_P}{2} \tag{3}$$

The mathematical-analytical results were found by computer-assisted integration using Derive (SoftWare House Inc.). The voluminous results were translated into a Pascal-Source and are used in a homemade Borland Delphi 6 (Borland Software Corporation) program, fitting the simulated chromatogram to the experimental chromatogram by minimizing the square error sum in a systematic search along the axes.

At the best fit, the program writes the retention times of the reactants t_R and t_P, respectively, as well as the dead-time related reduced rate constants $k_a[1 - (\lambda_o - \lambda_i)]t_0$ and $k_e t_0(\lambda_o - \lambda_i)$ into an Excel (Microsoft Corp.) readable text file.

Because of the principle of microkinetic reversibility, the retention-time related rate constants are different from each other in the presence of an enantiomeric environment, i.e., in the column:

$$\kappa_R = \frac{k_a t_0(1 - (\lambda_o - \lambda_i))}{t_R - t_E} \qquad \kappa_P = \frac{k_a t_0(1 - (\lambda_o - \lambda_i))}{t_P - t_E} \tag{4}$$

The holdup-time in the capillary t_E cannot directly be determined from the reaction chromatogram, but establishing the flow-rate independent on-column retention ratio

$$t_C = \frac{\mu_P}{\mu_R} \tag{5}$$

t_E can be calculated from the retention time of the reactant:

$$t_E = t_R \frac{t_P/t_R - \tau_c}{1 - \tau_c} \tag{6}$$

and the enantiomerization constant k_e in the well-defined achiral environment of the pure eluent is then:

$$k_e = \frac{k_e t_0(\lambda_o - \lambda_i)}{t_E} \tag{7}$$

RESULTS FROM NUMERICAL EVALUATIONS

Numerical reaction chromatograms were evaluated using a finite difference scheme similar to the Czok and Guiochon[7] algorithm. Figures 2–4 show that the evaluations from the finite difference method and the analytical equation are practically congruent for small and large conversions and also for considerable differences in the standard deviations.

As can be seen from Table 1, the good agreement between the given and the recalculated rate constants demonstrates the validity of our calculations. The small differences in the rate constants are, for some part, due to the numerical error in the finite difference method. But especially, the increasing difference in the apparent rate constants k_a with increasing conversions is also

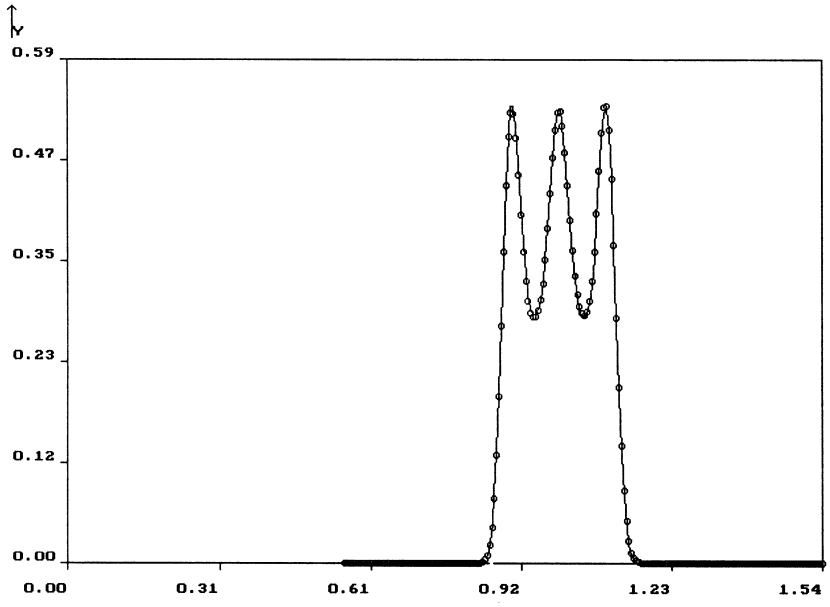

Figure 2. Recalculation of a numerical chromatogram with a high conversion (line: analytical approximation, circles: result of the finite difference calculation).

due to the limited precision of modelling a reversible reaction with 4 interconversions. For quantitative use the conversion should not exceed 50%.

RESULTS

The enantiomerization of oxazepam, which was thoroughly investigated by Cabrera and Schurig,[8] as well as Schoetz and Schurig[9] was used as a reference reaction.

The experiments were carried out with a modular HPLC from Knauer (Berlin, Germany) consisting of HPLC pump K-501, Knauer column oven, and DAD K-2700 WellChrom. Two ChiraDex 125×4.6 mm columns were connected by a 16 m (0.25 mm i.d.) capillary, and the whole setup was brought into the column oven. The eluent methanol/water (40/60, v/v) with 0.1% TEAA was used at pH 4.5. Investigations were carried out at 22, 25, and 28°C at 4 different flow rates. A typical result of the recalculations is shown in Fig. 5.

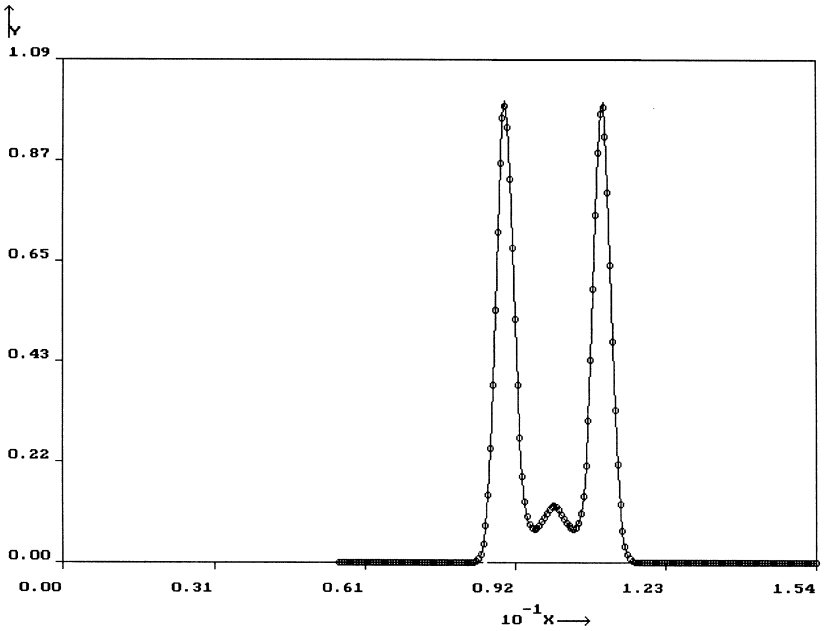

Figure 3. Recalculation of a numerical chromatogram with a low conversion (line: analytical approximation, circles: result of the finite difference calculation).

The apparent (on-column) rate constants κ_R and κ_P, as given in Tables 2 and 3, respectively, are in good agreement with each other, as well as with the data published by Cabrera[8] for the same column type and a similar eluent.

The rate constants in the pure eluent k_e (cf. Table 3) are larger and placed between data published by Aso[10] and by Yang.[11] The enantiomerization barriers of 90.5 kJ/mol for the on-column-process and 89.0 kJ/mol for the pure eluent are in good agreement with the data obtained by CE-investigations from Schoetz.[9]

CONCLUSIONS

The possibility to apply the simulated recyclization setup to complex reactions, especially to enantiomerizations, has been demonstrated. Rate constants can be obtained for the pure eluents (i.e., a well defined and homogeneous solvent) by a simple and rapid method. A disadvantage is that the high pressure on the "leading" column causes problems in the endurance

MARCEL DEKKER, INC. • 270 MADISON AVENUE • NEW YORK, NY 10016

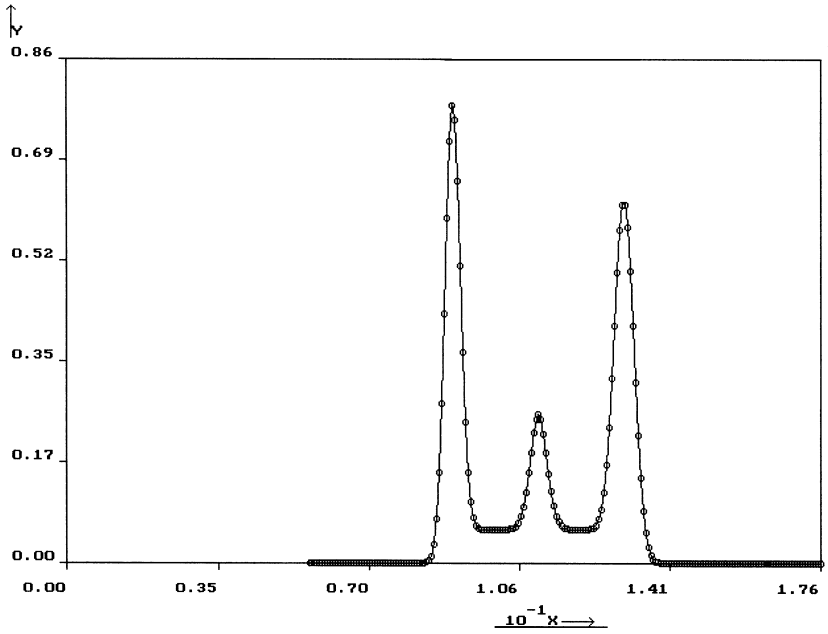

Figure 4. Recalculation of a numerical chromatogram with a moderate conversion and different standard deviations of the reactants (line: analytical approximation, circles: result of the finite difference calculation).

of the column, as well as the constancy of flow rates and retention times. However, these experimental problems might be overcome during further investigations. Meanwhile, the procedure has also been applied to reversible reactions with different rate constants, i.e., cis–trans-isomerizations.[12] The same fitting procedure can be applied, but the equilibrium constant in the eluent must be calculated from additional experiments without a capillary.

Table 1. Comparison of given and recalculated rate constants.

Chromatogram rate constant	I	II	III	IV	V
$k_{e\,\mathrm{recalc}}$	0.005	0.01	0.049	0.059	0.101
$k_{e\,\mathrm{given}}$	0.005	0.01	0.050	0.060	0.100
$k_{a\,\mathrm{recalc}}$	0.0150	0.0151	0.0154	0.0157	0.0746
$k_{a\,\mathrm{given}}$	0.0150	0.0150	0.0150	0.0150	0.0750

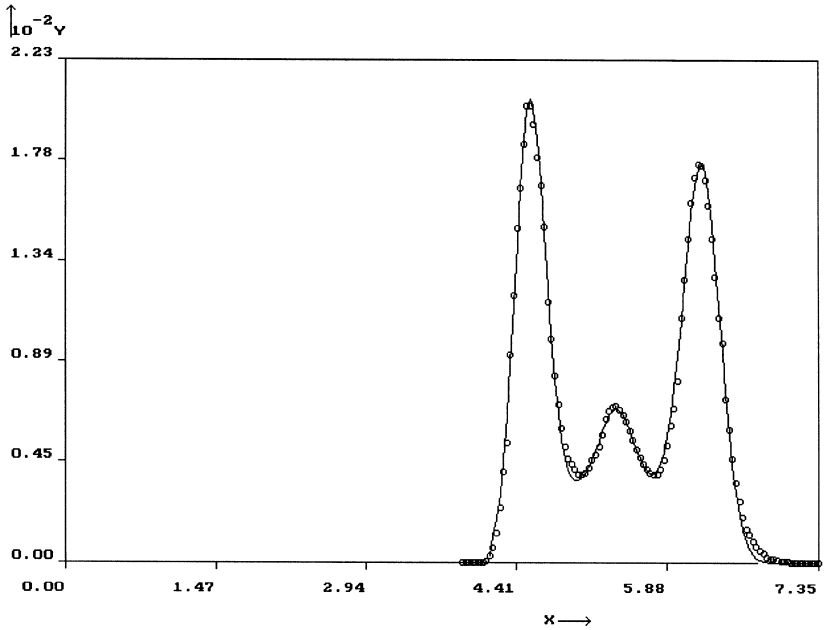

Figure 5. Typical result of the recalculation of an experimental chromatogram from the enantiomerization of oxazepam.

Also, from a direct comparison of simulated recycling and real recycling, it can be concluded that tolerances in columns lead to smaller errors than discontinuities in the flow rate, i.e., simulated recycling works at present better than real recycling. The method has a real potential in reaction kinetic investigations, however, there are two serious restrictions: First, in order to obtain unequivocal results, there must be some separation of the reactant primary peaks, which is a restriction for the eluent composition. Second,

Table 2. Rate constants from simple on-column measurement.

T (K)	κ_R (min$^{-1)}$	κ_P (min$^{-1)}$
295.15	0.028	0.042
298.15	0.040	0.059
301.15	0.057	0.083

Table 3. Rate constants from simulated recycling measurement.

T (K)	κ_R (min^{-1})	κ_P (min^{-1})	κ_e (min^{-1})
295.15	0.027	0.041	0.043
298.15	0.036	0.053	0.097
301.15	0.055	0.079	0.126

although the equation can be applied to capillary electrophoresis without problems, the method might not be.

ACKNOWLEDGMENT

The authors gratefully acknowledge financial support from the Deutsche Forschungsgemeinschaft (Proj. HA 2238/3-1).

REFERENCES

1. Trapp, O.; Schoetz, G.; Schurig, V. Determination of enatiomerization barriers by dynamic and stopped-flow chromatographic methods. Chirality **2001**, *13*, 403–414.
2. Bürkle, W.; Karfunkel, H.; Schurig, V. Dynamic phenomena during enantiomer resolution by complexation gas chromatography. J. Chromatogr. **1984**, *288*, 1–14.
3. Chu, A.H.T.; Langer, S.H. Void column liquid chromatographic reactor studies to determine reaction rates in mobile and stationary phases. J. Chromatogr. **1987**, *384*, 231–248.
4. Lange, J.; Haberland, D.; Thede, R. Determination of rate constants in a liquid chromatographic reactor with simulated recycling using empirical peak shape equations. J. Liq. Chromatogr. & Rel. Techniques **2002**, *17*, 2589–2600.
5. Thede, R.; Haberland, D.; Fischer, C.; Below, E.; Langer, S.H. Parametric studies on the determination of enantiomerization rate constants from liquid chromatographic data by empirical peak shape equations for multistep consecutive reactions. J. Liq. Chromatogr. **1998**, *21*, 2089–2102.
6. Thede, R.; Below, E.; Haberland, D.; Langer, S.H. Theoretical treatment of first-order reversible reactions occurring in a chromatographic reactor, on the basis of consecutive reactions. Chromatographia **1997**, *45*, 149–154.

7. Guiochon, G.; Czok, M. The physical sense of simulation models of liquid chromatography: propagation through a grid or solution of the mass balance. Anal. Chem. **1990**, *62*, 189–200.
8. Cabrera, K.; Jung, M.; Fluck, M.; Schurig, V. Determination of enantiomerization barriers by computer simulation of experimental elution profiles obtained by high-perfomance liquid chromatography on a chiral stationary phase. J. Chromatogr. A **1996**, *731*, 315–321.
9. Schoetz, G.; Trapp, O.; Schurig, V. Dynamic micellar electrokinetic chromatrography. Determination of the enantiomerization barriers of oxazepam, temazepam and lorazepam. Anal. Chem. **2000**, *72*, 2758–2764.
10. Aso, Y.; Yoshioka, S.; Shibazaki, T.; Uchiyama, M. The kinetics of the racemization of oxazepam in aqueous solution. Chem. Pharm. Bull. **1988**, *36*, 834–1840.
11. Yang, S.K.; Lu, X.-L. Resolution and stability of oxazepam enantiomers. Chirality **1992**, *4*, 443–446.
12. Lange, J.; Haberland, D.; Thede, R. Unpublished results, **2002.**

Received July 20, 2002
Accepted August 18, 2002
Manuscript 5915